

## Integrated analysis of light gauge steel beam sections enhanced by steel fiber reinforced concrete: a comprehensive study on structural and thermal performance

Christo George<sup>1</sup> , Subramanian Senthil Selvan<sup>1</sup> 

<sup>1</sup>SRM Institute of Science and Technology, College of Engineering and Technology, Department of Civil Engineering, Kattankulathur, 603203, Tamil Nadu, India.

e-mail: [senthils10@srmist.edu.in](mailto:senthils10@srmist.edu.in), [christychristo82@gmail.com](mailto:christychristo82@gmail.com)

### ABSTRACT

This study delves into the utilization of advanced materials to enhance the mechanical characteristics and longevity of concrete structures, with a specific focus on the performance and design of beams composed of light gauge steel hollow sections (LGSHS) filled with steel fiber-reinforced concrete (SFRC) under flexural conditions. SFRC, known for its exceptional fire resistance, emerges as a promising alternative to Ordinary Portland Cement (OPC) in elevating concrete properties. The experimental and numerical findings consistently demonstrated a noteworthy 12% increase in maximum loading capacity, exhibiting a consistent curved trend at the moment against mid-span displacement when employing the composite material. Finite Element Analysis (FEA) modeling was used to scrutinize core concrete failure patterns, residual displacements of external metal during the load-carrying process, and load distribution patterns throughout the structural element. The infusion of SFRC into light gauge steel sections was found to enhance load-carrying capacity, ductility, and toughness. This paper scrutinizes the mechanical properties and structural behavior of LGSHS filled with SFRC, encompassing steel and concrete properties, member geometry, and response to fire exposure. The primary objective is to assess the load-deformation characteristics of rectangular hollow beams formed by concrete-filled steel tubes (CFST) filled with SFRC. The investigation aims to determine load-carrying capacity, strain, deformation capacity, ductility, and failure characteristics under ambient and elevated temperatures.

**Keywords:** CFST Beams; Steel Fibers; Steel Fiber-Reinforced Concrete (SFRC); Finite element analysis (FEA); Ambient and elevated temperatures.

### 1. INTRODUCTION

In contemporary construction projects, builders have increasingly incorporated composite components such as Concrete-Filled Steel Tubes (CFST) in structures and roadways [1, 2]. Research has shown that these composite structural members (CFSTs) exhibit greater strength and flexibility than traditional steel tubing elements with similar forms and material properties [3, 4]. The enhanced performance is attributed to the concrete filling, which effectively minimizes or delays lateral deformation in elevated zones of the hollow members [1]. Moreover, CFST components have become more cost-effective by reducing labor and craftsmanship requirements, facilitating faster production, and contributing to overall cost reductions [5]. CFST components may undergo retrofitting or refurbishing like other structural elements for various reasons. This could involve upgrades to accommodate heavier loads or repairs due to aging, fire damage, or stress-related issues. Recent research investigations have explored the effectiveness of using polymer concrete and CFST hollow sections to enhance structural steel [6]. These studies have delved into different strengthening methods, load distribution, and the bonded behavior between steel substrates and Fiber-Reinforced Polymer (FRP) composites. Notably, experiments, including those cited in references [7–15], have consistently demonstrated the feasibility and advantages of employing CFST components to withstand various loads [16–22]. This growing body of research underscores the significance of CFSTs in contemporary construction practices, emphasizing their structural benefits, cost-effectiveness, and versatility in addressing different engineering challenges.

The absence of data on fire safety precautions for composite construction utilizing Concrete-Filled Steel Tube (CFST) components has been identified through both experimental studies [10, 11] and numerical analyses conducted by researchers [12]. While CFST components are widely recognized for their high fire resistance,

concerns arising from the adverse impact of the Kobe earthquake in 1995 on steel and concrete matrix composites, have led some scholars to question the use of conventional concrete as the infill material in steel tubes.

In response to these concerns and the need for a deeper understanding of the behavior of CFST rectangular beams filled with steel fiber-reinforced concrete under high temperatures, research initiatives have been initiated [23–25]. These investigations aim to shed light on the performance of CFST components in fire conditions, addressing the gap in knowledge and ensuring that appropriate fire safety precautions can be implemented in composite constructions involving CFST elements. The outcomes of such studies are crucial for establishing guidelines and best practices in the design and construction of CFST-based structures, particularly in the context of fire resilience.

Incorporating fibers into regular concrete has proven to be an effective method for enhancing its inherent fracture toughness. Fiber-reinforced concrete exhibits superior post-crack performance compared to plain concrete, as the fibers act to bridge fissures in the matrix and transmit impact stress to the substrate. For example, the presence of steel fibers across shear failure surfaces in steel fiber-reinforced concrete enhances shear internal friction when diagonal tension cracks appear. This improves shear transmission across fault planes, leading to a finer decline in axial load [26].

The addition of fibers enhances post-crack performance and increases load-bearing capacity, flexibility, and tensile strength [27]. Various parameters, including matrix strength, fiber volume, and fiber surface support and interaction, influence these characteristic improvements [28, 29]. Recent research has focused on confirming the efficacy of fiber reinforcement in improving fire resistance [30–34]. 1% of Steel fibers are commonly incorporated into contemporary construction methods, often in conjunction with conventional reinforcement bars or rolled steel profiles. Incorporating steel fibers into the concrete mix augments the tensile, compressive, and ductile strengths of concrete at ambient temperatures. Many research endeavors have investigated the behavior of fiber-reinforced concrete (FRC) when exposed to elevated temperatures. This underscores the paramount importance of evaluating fire resistance in structural components.

In the context of light gauge steel beams, studies have investigated the flexural behavior of beams filled with steel fiber-reinforced concrete. Findings indicate that such beams exhibit improved flexural strength and stiffness compared to conventional concrete-filled beams [35–37]. The amount of steel fiber content in the concrete infill has been identified as a critical factor influencing the flexural strength and stiffness of light gauge steel beams. Additionally, under static and dynamic loading conditions, light gauge steel beams filled with steel fiber-reinforced concrete have demonstrated superior performance, stiffness, and ductility compared to conventional concrete-filled beams [38–41]. Moreover, the use of steel fiber-reinforced concrete as infill material in light gauge steel beams has been found to enhance their fire resistance, leading to longer fire resistance times [42]. Performing a strain gauge test on a beam involves attaching strain gauges to the surface of the beam to measure the strain induced by applied loads. This type of testing provides valuable information about the structural behavior and performance of the beam under different conditions.

While Concrete-Filled Steel Tube (CFST) sections are commonly used in composite construction, existing design requirements lack coverage of the fire resistance of these sections and related safety precautions. Following the Kobe earthquake 1995, questions have arisen about using steel tubes despite their considerable fire resistance. This research aims to investigate the underlying behavior of post-fire CFST rectangular beams filled with Steel Fiber-Reinforced Concrete (SFRC) of different grades (M20, M30, and M40) in both service load and ultimate state conditions. Theoretical strength values were determined using the American Standard Code of Practice. The primary goal is to contribute to enhancing fire safety measures in structures incorporating CFST components.

## 2. MATERIALS AND METHODS

### 2.1. Materials properties

The CFST beams in this study were constructed using hollow steel tubes with rectangular cross-sections. For each tube form, three samples were cut and processed for the flexural test by ASTM-E8/E8 M-09 standards [43]. The characteristics of the steel tubes were evaluated by examining samples, with the mean findings of three specimens presented for each tube form in Table 1. The primary objective of the study was to assess the load-deformation of hollow section beams made of CFST Infilled with steel fiber-reinforced concrete (SFRC) of different concrete grades, namely M20, M30, and M40 [44]. The material properties of the rectangular steel tubes are provided in Table 2, offering key insights into the components used in constructing the CFST beams. The experimental setup, conducted in accordance with ASTM standards, ensures reliable and standardized testing procedures for the evaluation of the beams' flexural behavior and load-deformation characteristics.

**Table 1:** Descriptions of the beam specimens.

BEAM ID	DESCRIPTION
AT- AMBIENT TEMPERATURE	
B-AT	Ambient temperature hollow beam
B-M20-CC-AT1	Concrete at ambient temperature and a standard M20 grade infill beam
B-M20-SFRC-AT2	M20 grade steel fiber reinforced concrete infill beam at ambient temperature
B-M30-CC-AT1	M30 grade conventional infill beam, ambient temperature concrete
B-M30-SFRC-AT2	At ambient temperature, M30 grade steel fiber reinforced concrete infill beam
B-M40-CC-AT1	Conventional concrete infill beams of M40 grade at room temperature
B -M40-SFRC-AT2	A beam made of M40-grade steel fiber reinforced concrete is kept at ambient temperature.
ET- ELEVATED TEMPERATURE	
B-ET	Beam hollow at elevated temperatures
B-M20-CC-ET1	Standard M20 grade concrete infill beam at elevated temperatures
B-M20-SFRC-ET2	At elevated temperatures, M20 grade steel fiber reinforced concrete infill beam
B-M30-CC-ET1	Conventional concrete infill beams of M30 grade at elevated temperatures
B-M30-SFRC-ET2	At elevated temperatures, M30 grade steel fiber reinforced concrete infill beam
B-M40-CC-ET1	Conventional concrete infill beams of M40 grade at elevated temperatures
B-M40-SFRC-ET2	At elevated temperatures, M40 grade steel fiber reinforced concrete infill beam

**Table 2:** Material properties of rectangular steel tubes.

MATERIAL PROPERTIES	RECTANGULAR LIGHT GAUGE STEEL TUBES
Size (mm)	Size = 100 × 50, Length = 750, thickness = 2
Elastic limit $f_y$ (MPa)	450
Maximum strength $f_u$ (MPa)	489
Elongation (%)	15.4
Poisson's ratio	0.27
Modulus of Elasticity $E_s$ (N/mm <sup>2</sup> )	210,000

## 2.2. Steel and steel fibre properties

This investigation used crimped steel fibers that conform to ASTM A820-01 [45]. Table 3 shows the properties of steel fibers used in the present study.

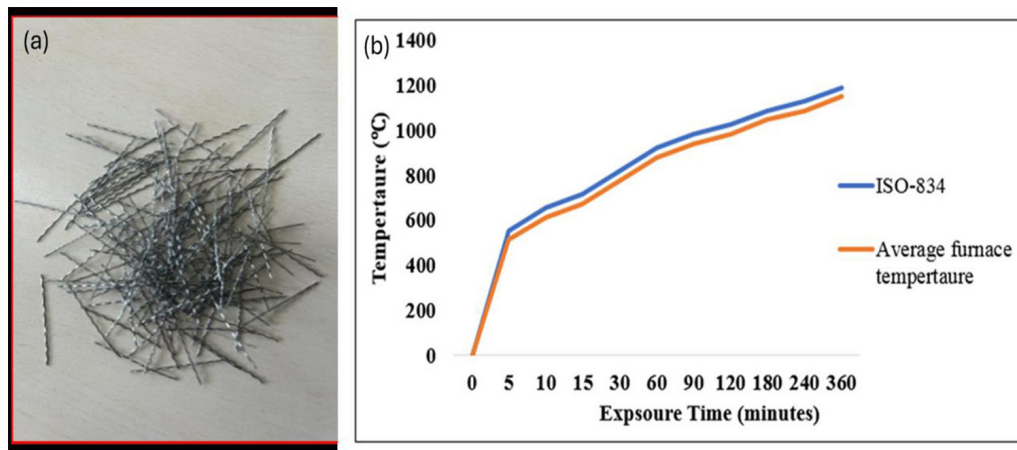
In the investigation mentioned, crimped steel fibers were employed. Crimped fibers have a wavy or zigzag shape, contributing to improved bonding between the fibers and the concrete matrix. This enhanced bond is instrumental in further elevating the mechanical properties of the concrete. The crimped shape allows for better interlocking between the fibers and the surrounding concrete, providing additional reinforcement. A 1% of steel fibers are used for the grades and 24.55 kg/m<sup>3</sup> of steel fiber quantity was estimated.

Notably, deformed fibers, such as crimped ones, typically come in bundles and exhibit a more intricate shape than round or rectangular fibers. This complexity in shape contributes to a more effective distribution of stress within the concrete matrix, ultimately leading to improved tensile strength, ductility, and crack control. The choice of fiber shape and type is often tailored to the specific requirements of the concrete application and the desired performance characteristics of the structure.

In all cases, steel tubes were cold-produced from steel plates through press bends and joint welding. Tensile testing was conducted on steel coupons extracted from the standard tubes. The 0.2% elastic stress was employed, as indicated in the literature for cold-formed and hot-formed steel tubes. Figures 1a and 1b illustrate the steel fibers and the ISO-834 fire curve, conforming to the relevant code or standards. These tests and analyses provide valuable insights into the mechanical properties of the steel tubes, aiding in assessing their structural performance and suitability for specific applications.

**Table 3:** Properties of steel fibre.

PROPERTIES	ROUND CRIMPED STEEL FIBRE
Density	7680 kg/m <sup>3</sup>
Tensile strength	1100 (MPa)
Elastic modulus	$2.1 \times 10^5$ N/mm <sup>2</sup>
Specific gravity	7.9
Length of steel fibre	30 mm
Diameter of steel fibre	0.50 mm
Aspect ratio of steel fibre	60
ASTM specs	ASTM A820 M04 [TYPE-I]

**Figure 1:** (a) Steel fibers; (b) furnace temperature vs. ISO-834.

### 2.3. Preparation of specimen

CFST is typically made up of hollow steel tubes, the strength of concrete, super softener or other alloying elements, and moisture, among other things, with the concrete hollow section being the two most important components. Average-strength concrete is used in most CFSTs. The materials and mechanical qualities of CFST made from the above-mentioned concretes can be improved further when subjected to higher temperatures. The increased strength of concrete greatly increases the stiffness, stress capacity, or current capabilities of CFST beams.

### 2.4. Preparation of concrete

In the investigation, OPC 53-grade cement was utilized as the binding material. This type of cement, categorized as Ordinary Portland Cement (OPC), is distinguished by its elevated compressive strength compared to other OPC varieties [46–48]. The cement's loss of ignition value, measured at 0.98, denotes the proportion of volatile materials lost during heating. Additionally, the specific gravity of 3.15 indicates the density of the Cement. For fine aggregate, locally available river sand conforming to grading zone-II of IS: 383-2016 was employed. This grading zone signifies that the sand possesses a particle size distribution suitable for concrete production. The sand is finely textured and passes through a sieve with a 4.75 mm opening. The fineness modulus, with a value of 2.57, provides information about the particle size distribution of the sand. A higher fineness modulus indicates a coarser particle size distribution. The mix proportions for different grades of concrete are outlined in Table 4, following the guidelines of IS 10262:2019. The specific gravity of the sand, measured at 2.71, signifies its density relative to water. The chemical composition of the cement reveals a calcareous part of around 70% and an argillaceous part of about 30%, indicating favorable mechanical properties. These material specifications ensure the concrete mix is designed with appropriate ingredients to meet the desired performance and structural requirements.

The coarse aggregate employed in the investigation is a well-graded angular granite stone with a maximum/minimum size of 20 mm and 10 mm, conforming to the specifications outlined in IS: 383-1970 [47].

This adherence to standards ensures that the stone possesses a particle size distribution suitable for concrete production. The angular shape of the stone is advantageous as it can provide better interlocking and bonding with the cement paste, thereby enhancing the strength and durability of the concrete.

The specific gravity of the granite stone, measured at 2.7, indicates its density relative to water. A higher specific gravity value suggests the stone is denser, while a lower value indicates a lighter stone. In this case, the specific gravity of 2.7 means a moderately dense stone. The fineness modulus, recorded at 7.2, provides information about the particle size distribution of the coarse aggregate. A higher fineness modulus indicates a coarser particle size distribution. The use of well-graded angular granite stone in the concrete mix contributes to achieving the desired structural properties and overall performance of the concrete.

### 2.5. Light gauge steel sections

Figure 2 illustrates a 2 mm thick steel tube with a specified yield strength ( $f_y$ ) of Light Gauge Steel at 236.843 N/mm<sup>2</sup> and an ultimate tensile strength ( $f_u$ ) of Light Gauge Steel at 388.053 N/mm<sup>2</sup>. Notably, the minimum yield strength of Light Gauge Steel ( $f_y$ ) according to IS: 801-1975 is stipulated as 210 N/mm<sup>2</sup>.

The yield strength and tensile strength of the Concrete-Filled Steel Tube (CFST) were determined through conventional tensile testing methods. These tests provide crucial information about the mechanical properties of the steel tube, such as its ability to withstand loads and deformation. The measured values are compared against industry standards and specifications, ensuring the steel tube meets the required strength criteria outlined in relevant codes and guidelines. This rigorous testing process is essential for verifying the structural integrity and performance of the CFST steel tube in various applications. The foil-type strain gauge used a resistance of 120 OHM and an active length of 5 mm.

### 2.6. Analytical techniques of steel tube

Predicated on the dimensional properties of CFST, a 3-dimensional polyhedral aspect and a triangular-shaped lowered shell component for concrete and a triangular-shaped first-order lowered shell component for pipe are selected, respectively. Pinned conditions were given at the ends of the beam at the bottom of the steel tube. Steel tube is loaded from the top. Figure 3 depicts the design parameters and geometry of the FEA modeling.

**Table 4:** Mix the composition of concrete.

TYPE OF GRADE	C	FA	CA	RATIO OF WATER TO CEMENT
M20	1	2.704	4.271	0.54
M30	1	1.807	3.529	0.43
M40	1	1.749	3.491	0.40

C-Cement; FA- Fine aggregate; CA-Coarse aggregate.



**Figure 2:** Light gauge steel tube and tensile coupon test.

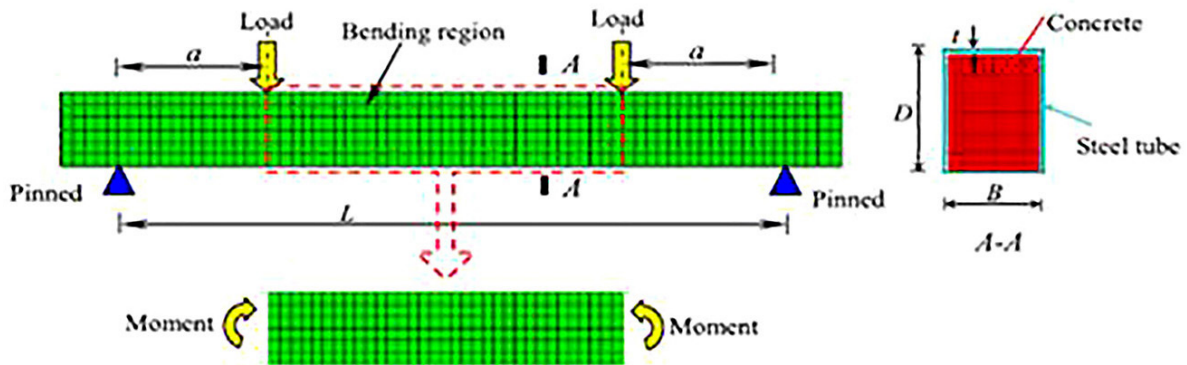


Figure 3: Boundary and mesh conditions.

### 3. RESULTS AND DISCUSSION

#### 3.1. Mechanical properties

The Concrete-Filled Steel Tube (CFST) specimens in the investigation exhibit shear failure in the concrete, as observed in the results presented in Figures 4, 5, and 6. Following the removal of the external hollow steel specimen, clear evidence of maximum compressive, flexural, and split tensile tests in concrete is evident among the thickenings.

Figure 4, which likely corresponds to the compressive test, shows the behavior of the concrete under axial load. The emergence of the primary diagonal crack aids in the decrease of axial load. The principal mechanism for sustaining resistance to imposed axial load in plain concrete involves force transmission through shear on the broken surfaces.

Similarly, Figure 5, likely representing the flexural test, illustrates the concrete's response to bending forces. The visible patterns and characteristics provide insights into the flexural behavior of the concrete within the CFST specimen.

Figure 6, corresponding to the split tensile test, captures the behavior of the concrete under tensile forces. The observations from these tests collectively contribute to a comprehensive understanding of the mechanical performance of the CFST specimens, especially in terms of compressive, flexural, and tensile strengths. These findings are crucial for assessing the structural behavior and integrity of CFST elements in practical applications.

The results indicate that the compression, split tensile, and flexural strength of M20, M30, and M40 concrete containing steel fibers decreases as the temperature increases. The behavior of CFST (Concrete-Filled Steel Tube) samples at elevated temperatures is similar to that observed in ambient temperature specimens. This similarity in failure mode is attributed to the fundamental role of steel fibers in creating a shearing plane in the structural frame.

The presence of steel fibers delays the development of bulging in the CFST specimens at elevated temperatures. This delay results from the steel fibers restraining the movement across opposing slide planes, alleviating the stresses on the external steel section due to cement expansion. Despite the elevated temperature, CFST samples exhibit a milder reduction in axial stress. The maximum stress is the maximum pressure during unloading, and the flexural strength of CFST samples tends to be in the middle to upper range. The effects of challenging conditions and metal attributes on the maximum stress of CFST samples align with expectations. As the ambient sample compressive strength increases, so does the final load. With increasing elevated temperature, there is a corresponding increase in load capacity. However, the elevated temperature only slightly influences the ultimate load of the CFST specimens. Comparing the standard CFST ambient samples with those subjected to elevated temperatures (0.7%, 0.8%, and 1.3%), there is an improvement in ultimate load by 3.0–7.0%, 5.0–11%, and 6.0–15.0%, respectively. This suggests that incorporating steel fibers in CFST specimens contributes to enhanced performance, even under elevated temperature conditions, improving load-bearing capacity.

#### 3.2. Load-carrying capacity of concrete at ambient and elevated temperatures

Figure 7 illustrates that the structural performance of a beam can vary significantly between ambient and elevated temperatures. At ambient temperatures, the beam undergoes various loading conditions, such as bending and

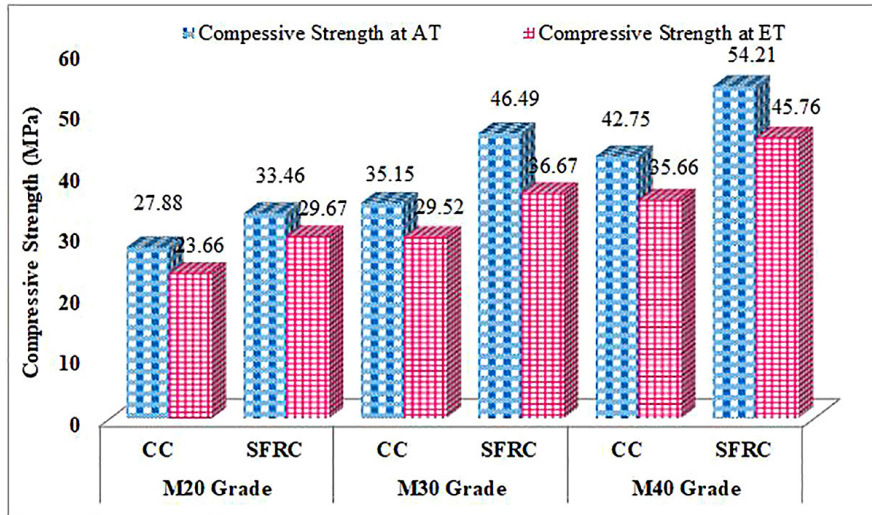


Figure 4: Compression strength of concrete at ambient and elevated temperatures.

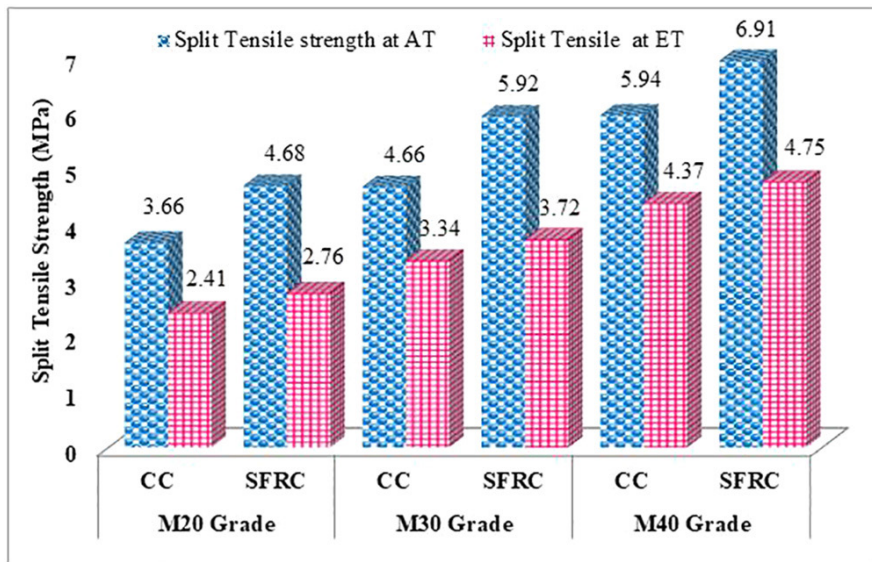


Figure 5: Split tensile strength of concrete at ambient and elevated temperatures.

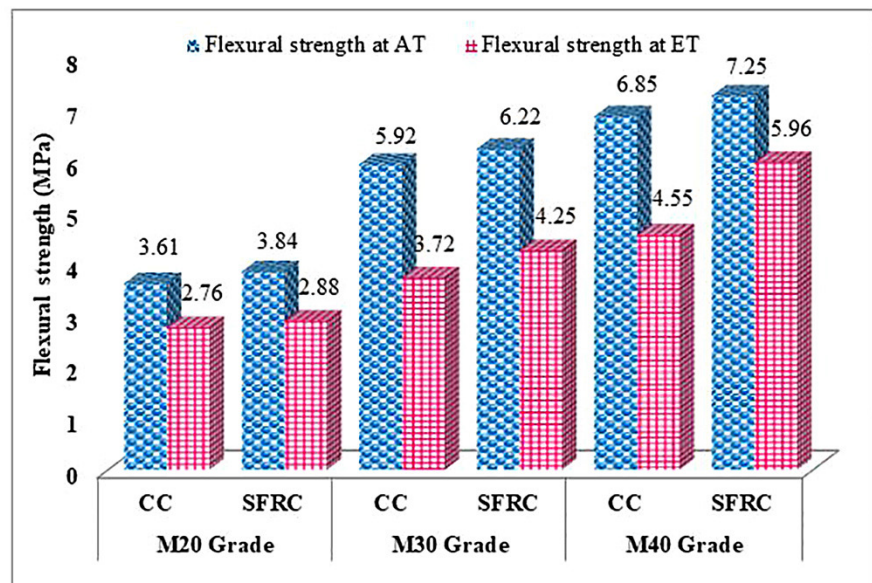


Figure 6: Flexural tensile strength of concrete at ambient and elevated temperatures.

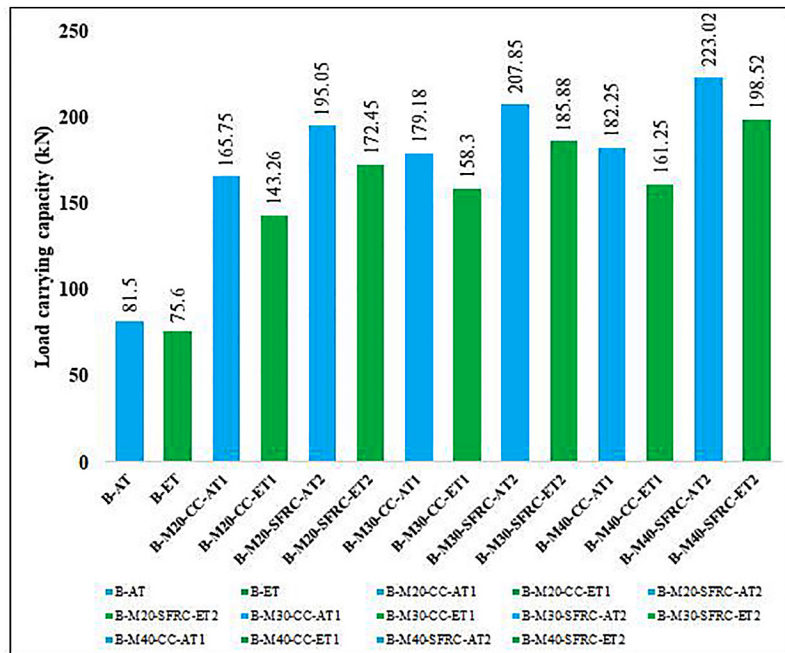


Figure 7: Load-carrying capacity of the CFST rectangular beam (ambient & elevated temperatures).

shear, and its performance is typically characterized by factors like strength, stiffness, and ductility. However, when exposed to elevated temperatures, the structural behavior of the beam is influenced by factors including thermal expansion, dehydration, and chemical changes. Elevated temperatures can substantially impact the beam, potentially causing significant damage and reduced strength, stiffness, and ductility. The exposure to elevated temperatures affects different types of beams, including hollow beams, conventional concrete-filled beams, and steel fiber concrete-filled beams. Understanding how these beams respond under elevated temperature conditions is crucial for ensuring the safety and reliability of structures in fire scenarios or other situations involving high temperatures. The investigation in Figure 7 is likely presents data or graphs depicting the comparative performance of these beams under different temperature conditions.

The load-carrying capacity reduction of concrete-filled beams with different grades and reinforcement types when exposed to elevated temperatures. The percentage reductions in load-carrying capacity for other grades are as follows:

1. M30 grade conventional concrete-filled beam: 11.85% reduction.
2. M40 grade conventional concrete-filled beam: 14.66% reduction.
3. M20 grade steel fibre reinforced concrete-filled beam: 7.98% reduction.
4. M30 grade steel fiber-reinforced concrete-filled beam: 9.4% reduction.

The load-carrying capacity values obtained experimentally for the beams were compared with theoretical values proposed by various codes such as EC-EN 1994-1-2005, ANSI/AISC 360-16, AIJ-97, and BS 5950-5-2000.

This suggests that the experimental outcomes are better than the predictions made by these codes, indicating that they are reliable for determining the load-carrying capacity of similar structural beams. However, it is important to note that there may be variations in the results depending on the specific conditions and materials used in the experiment.

### 3.3. Comparison of test results with standard codes

Experimental analysis and results for rectangular Concrete-Filled Steel Tube (CFST) beam specimens, categorized into Group 1 (Ambient temperature) and Group 2 (Elevated temperature). The analysis involves a comparison of four major parameters based on different design codes: EC-EN 1994-1-2005, ANSI/AISC 360-16, AIJ-97, and BS 5950-5-2000.

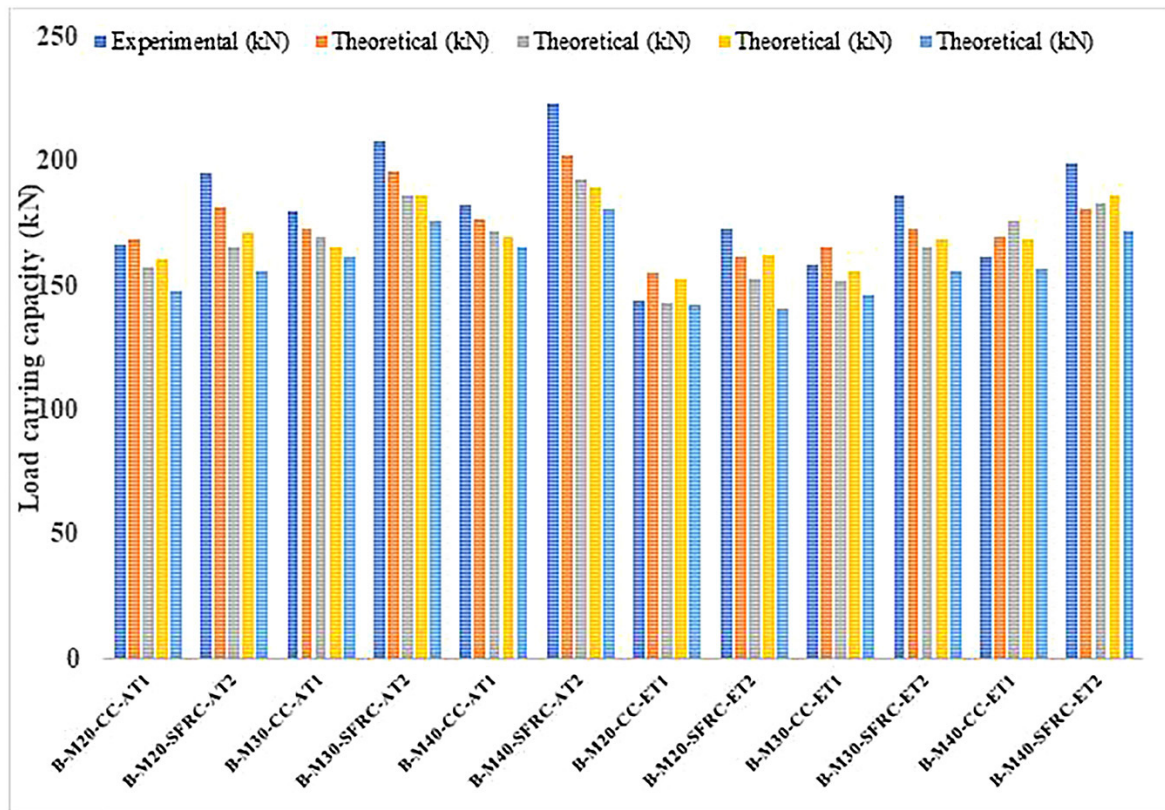


Figure 8: CFST beams (ambient & elevated temperatures).

For each of the seven beam specimens, the loads are measured at yield and ultimate stages, recorded in kilonewtons (kN), and deflections are measured in millimeters. Figure 8 provides a comparative representation of the ultimate loads of each rectangular CFST beam specimen at both ambient and elevated temperatures. The computed values are derived from the specified design codes, and the percentage difference is illustrated compared to the experimental ultimate loads.

This comprehensive analysis and comparison allow for assessing how well the CFST beams perform under different conditions, providing insights into their behavior and validating the experimental results against established design codes. The percentage difference helps gauge the accuracy and reliability of the design codes in predicting the ultimate loads of the CFST beams in both ambient and elevated temperature scenarios.

### 3.4. Load vs. deflection characteristics of the beam at ambient and elevated temperatures

At ambient and elevated temperatures, the load Vs. The deflection curve typically shows a linear region up to a certain load, as shown in Figure 9, after which the deflection increases rapidly with a relatively constant load. This indicates the onset of yield and plastic deformation of the beam. The load Vs. The deflection curve at elevated temperatures may show a similar trend. Still, the onset of plastic deformation and failure may occur at lower loads and deflections due to the effects of thermal degradation.

The load-deflection characteristics of the beam were investigated under both ambient and elevated temperatures, as depicted in Figure 10. A deflectometer was utilized to measure deflection in both the x and y directions. The load-deflection plots exhibited three distinct zones: a non-linear transition stage connecting two linear stages (the first and third regions) and the second region.

In the load-deflection plots, the first section is primarily influenced by the behavior of the concrete core, showcasing non-linear characteristics. The transition stage connects this non-linear region to the second region, where the load-deflection relationship becomes more linear. In this second region, the load is distributed between the concrete core and the steel tube.

The dominance of the steel tube characterizes the third region of the load-deflection plot, showcasing its strength as the primary structural element. This three-zone behavior highlights the interaction between the concrete and steel components of the beam under different loading conditions.

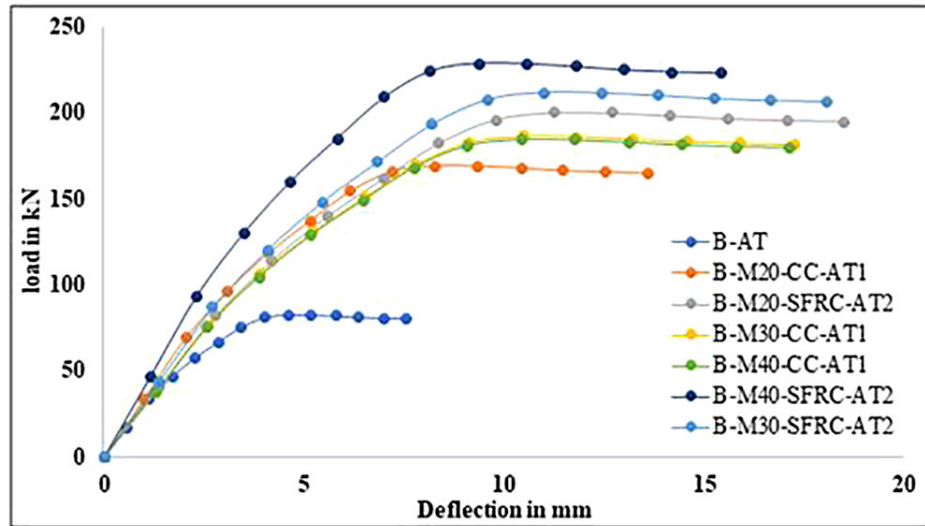


Figure 9: Load vs. deflection at ambient temperature in beams.

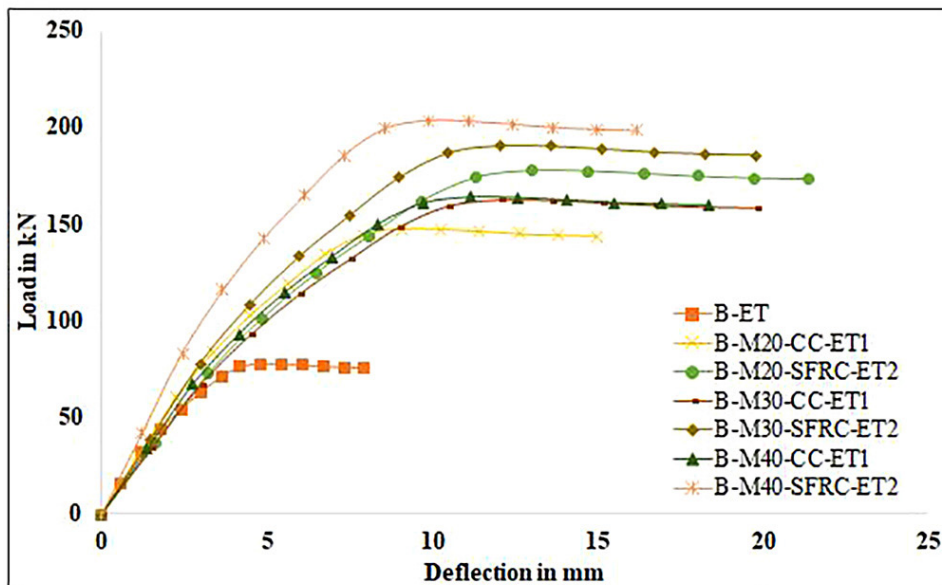


Figure 10: Load vs. deflection at elevated temperature in beams.

Furthermore, a hollow beam's load vs. strain characteristics in tensile loading were analyzed, as depicted in Figure 11. This analysis provides insights into how the beam responds to tensile forces and the corresponding strain development along its length.

At ambient temperature, these characteristics are linear up to the point of yielding, after which the curve becomes non-linear. The strain exhibits exponential growth as the load increases until the beam fails. Similarly, in compressive loading, the load vs. strain characteristics are linear up to yielding, and the curve becomes non-linear. At elevated temperatures, the load vs. strain characteristics in both tensile and compressive loading are influenced by the material's thermal expansion, as depicted in Figure 12. The beam undergoes expansion, causing the load vs. strain curve to shift upwards. Additionally, the material properties of the beam can change at elevated temperatures, further impacting the load vs. strain characteristics. The strain behavior of the beam specimen is examined after exposure to ambient and elevated temperatures. This analysis provides valuable insights into the hollow beam's thermal behavior and mechanical response under different loading conditions and temperatures.

### 3.5. Ductility ratio of concrete

The ductility ratio of a beam, as defined in reference [45], is calculated by taking the ratio of the deflection at the ultimate limit state to the deflection at the breaking point. It serves as a measure of the beam's ability to deform without collapsing, providing insights into its ductile behavior. The ductility ratio is influenced by a range of factors, including material properties, dimensions, boundary conditions, loading conditions, and temperature, as noted in reference [49]. From the information presented in Table 5, it is evident that the ductility ratio of a Concrete-Filled Steel Tube (CFST) concrete-filled beam is generally higher than that of a hollow beam. This implies that the CFST concrete-filled beam exhibits better ductility than its hollow counterpart. The enhanced ductility can be attributed to the interaction between the steel tube and the concrete core in CFST beams, contributing to a more robust and ductile structural response.

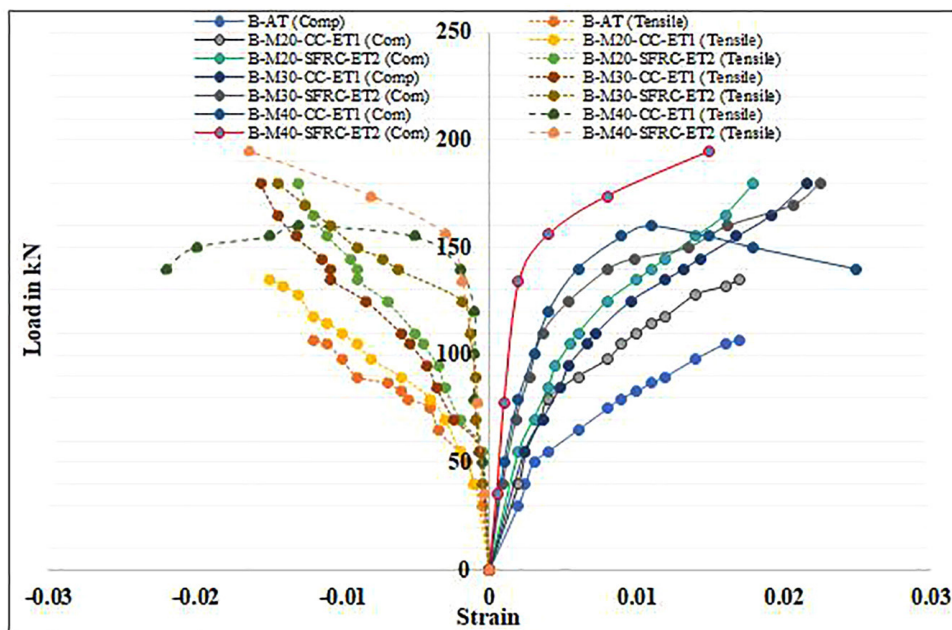


Figure 11: Load vs. strain at ambient temperature in beams.

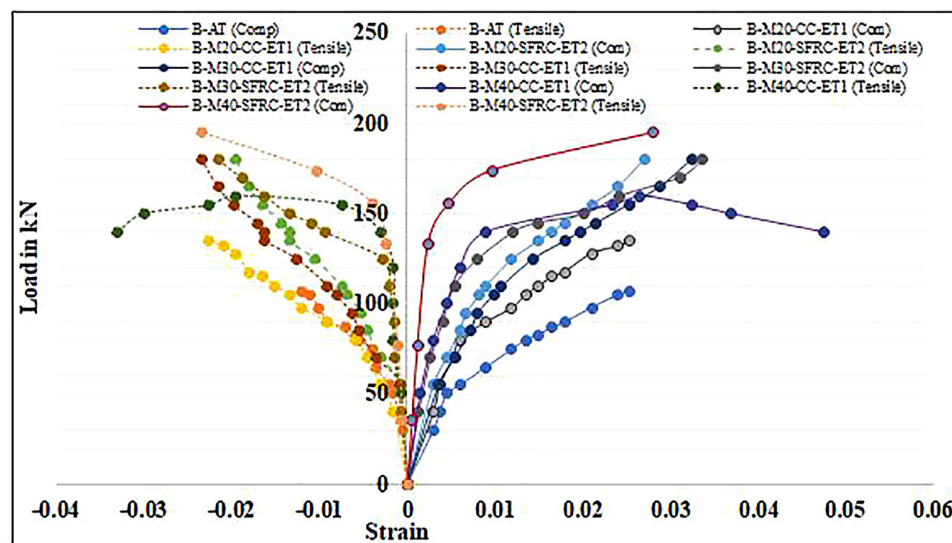


Figure 12: Load vs. strain at elevated temperature in beams.

**Table 5:** Ductility ratio of beams.

BEAM ID	VALUES
B-AT	1.01
B-M20-CC-AT1	1.09
B-M20-SFRC-AT2	1.07
B-M30-CC-AT1	1.05
B-M30-SFRC-AT2	1.02
B-M40-CC-AT1	1.01
B-M40-SFRC-AT2	1.01
B-ET	1.10
B-M20-CC-ET1	1.11
B-M20-SFRC-ET2	1.09
B-M30-CC-ET1	1.08
B-M30-SFRC-ET2	1.06
B-M40-CC-ET1	1.07
B-M40-SFRC-ET2	1.09

### 3.6. Failure modes

The failure mode of a hollow beam at ambient temperature is typically bending, given the lower strength and stiffness of the material, making it more susceptible to deformation. In elevated temperatures, the material's thermal expansion can cause the beam to bend or deform earlier, leading to failure. Additionally, the reduction in the ultimate strength and stiffness of the material can contribute to failure, either in bending or shear, as shown in Figure 13. The introduction of concrete provides additional confinement to the steel, enhancing both the strength and stiffness of the beam. This additional confinement helps to mitigate the susceptibility to bending or shear failure. However, it's important to note that the failure mode of the beam can still occur in bending or shear if the loading conditions exceed the capacity of the beam, even with the presence of concrete. At elevated temperatures, the decrease in the strength and stiffness of the concrete can become a significant factor contributing to the failure mode of the beam. The combination of thermal effects on both the steel and concrete components influences the overall behavior of the hollow beam, making it essential to consider these aspects in the design and assessment of structures exposed to elevated temperatures.

### 3.7. Numerical investigation

In the Finite Element Analysis (FEA) modeling described, a first-order lowered 3D hexahedral solid element was chosen for concrete, and a triangular-shaped first-order lowered shell component was selected for steel tubes in the rectangular Concrete-Filled Steel Tube (CFST). The composite parameters were applied to represent the behavior of the CFST structure. Pinning initial conditions were specified near the end of the beam, just at the bottom of the concrete tube. The force was transmitted to the top of the steel tube.

To assess the usual failure patterns under various load mechanisms, stresses were applied at the two end parts of the bent region. This FEA modeling was validated using several beam tests described in reference [50]. The load against displacement curves, along with the failure mechanisms of the CFST samples, were compared between experimental results and predictions.

Figure 14 likely illustrates the geometry or meshing of the first-order lowered 3D hexahedral solid element used in the FEA analysis. The choice of appropriate elements and accurate modeling parameters is crucial for obtaining reliable predictions and insights into the behavior of the CFST structure under different loading conditions. The validation against experimental results enhances the confidence in the accuracy and applicability of the FEA model in simulating the structural response of CFST beams.

### 3.8. Analysis of the beam behavior

The load of cementitious materials at tensile is greater than the strength of cracking of concrete described in [51] and the initial breaking on the tensile side.

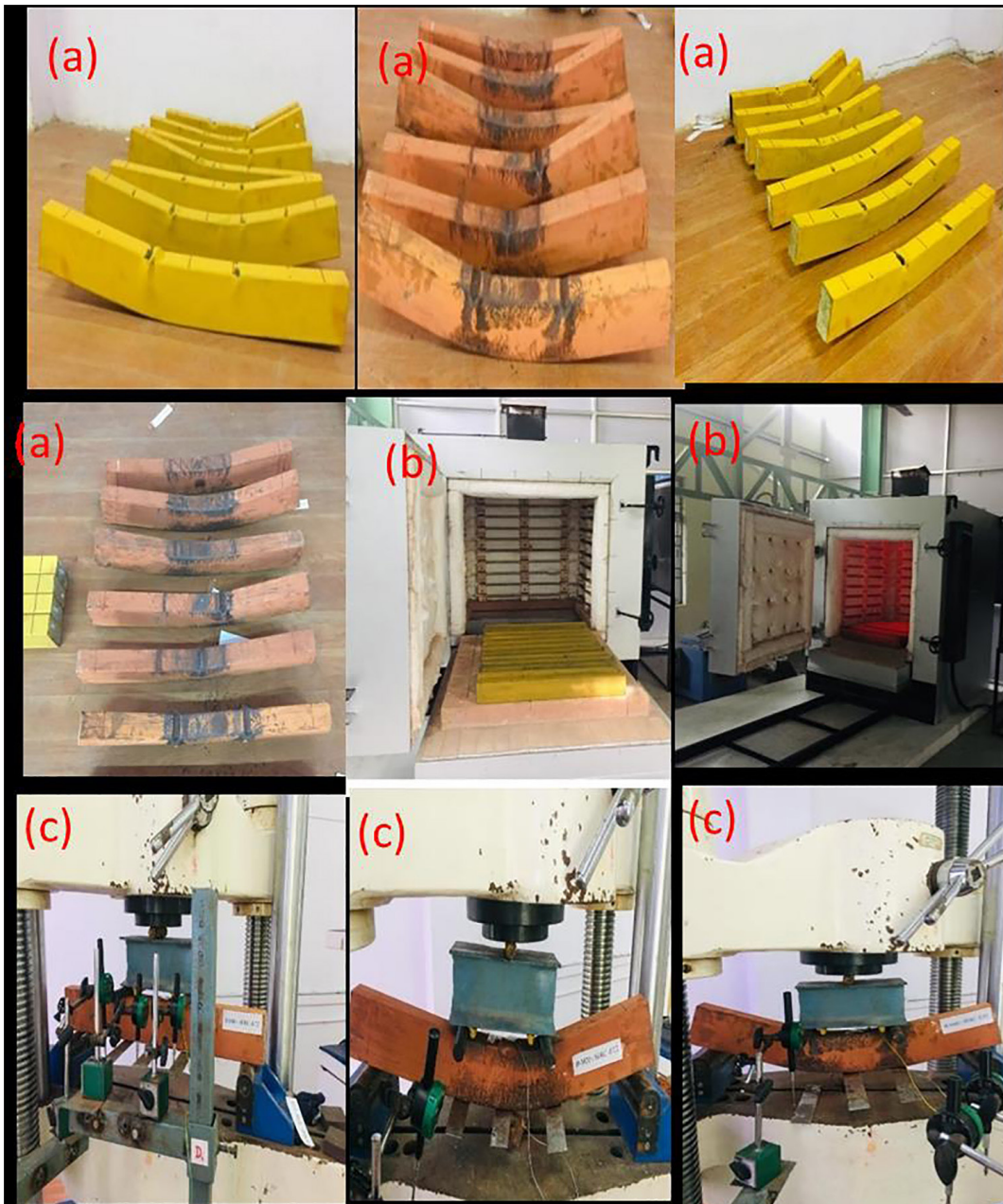


Figure 13: (a) CFST tested samples (b) elevated temperature (c) failure of the beams (ambient and elevated temperature).

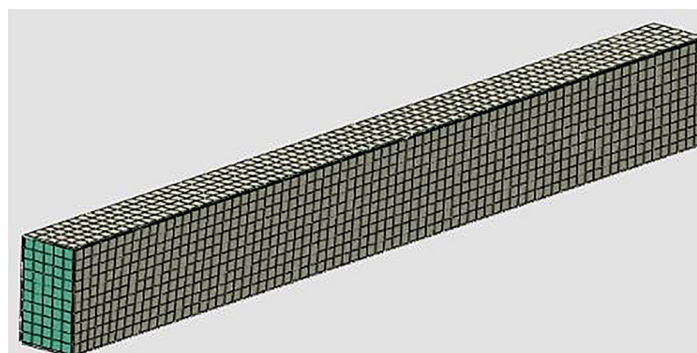


Figure 14: Mesh generation of beam.

### 3.9. Failure mode

As shown in Figure 15, the empty steel hollow section fails because the hollow section beam is caused by the compressive region (a). In the same period, as noted [52], in-filled cement, on the other hand, efficiently avoids bending and localization of hollow steel portions in CFST beams. As demonstrated in Figure 16, the inner concrete supports the steel hollow portion to resist local longitudinal distortion (b). As a result, steel's transverse flexibility can be fully realized. Such extensive plasticity formation in a composite is crucial for the capacities and flexibility of rectangle CFST beams.

Figure 17 depicts the evolution of the tensile deformation of the ductility of composite rectangular CFST beam. It was found that at the moment in time, the maximum possible value of both elastic deformations is

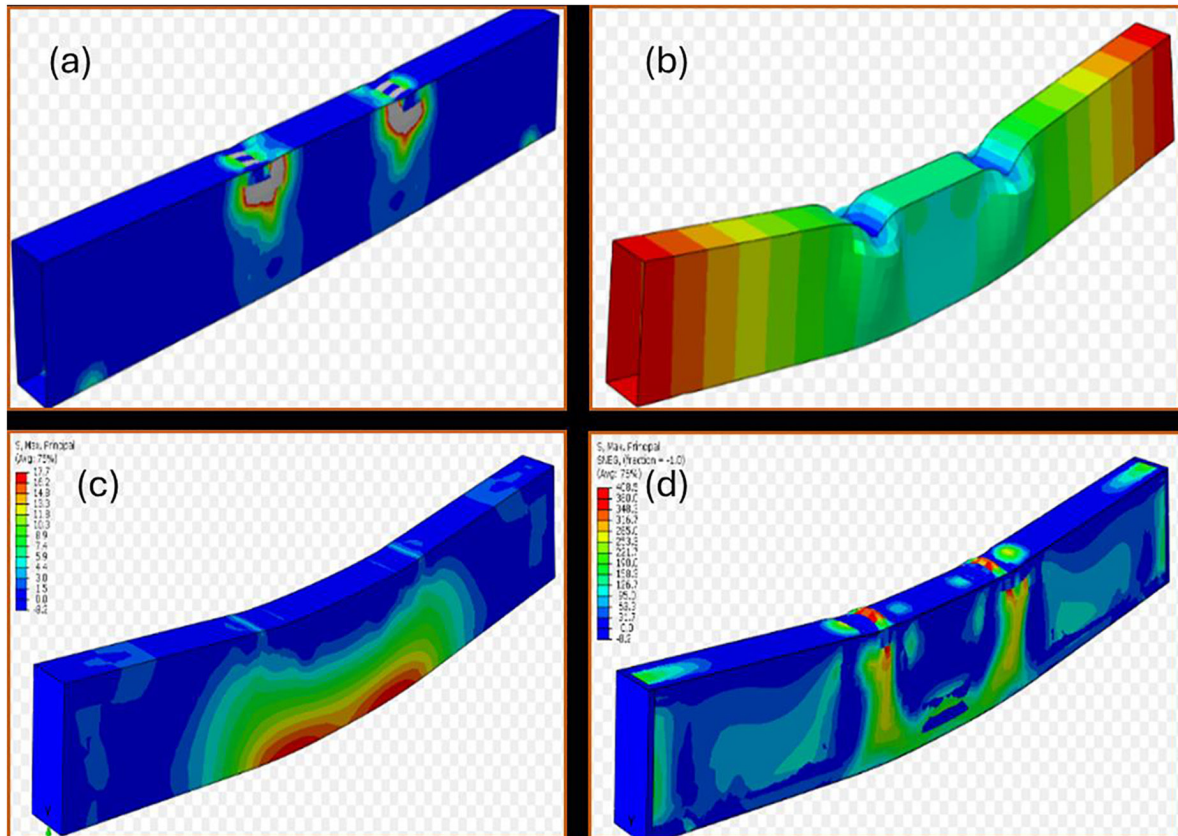


Figure 15: Failure mode of beam.

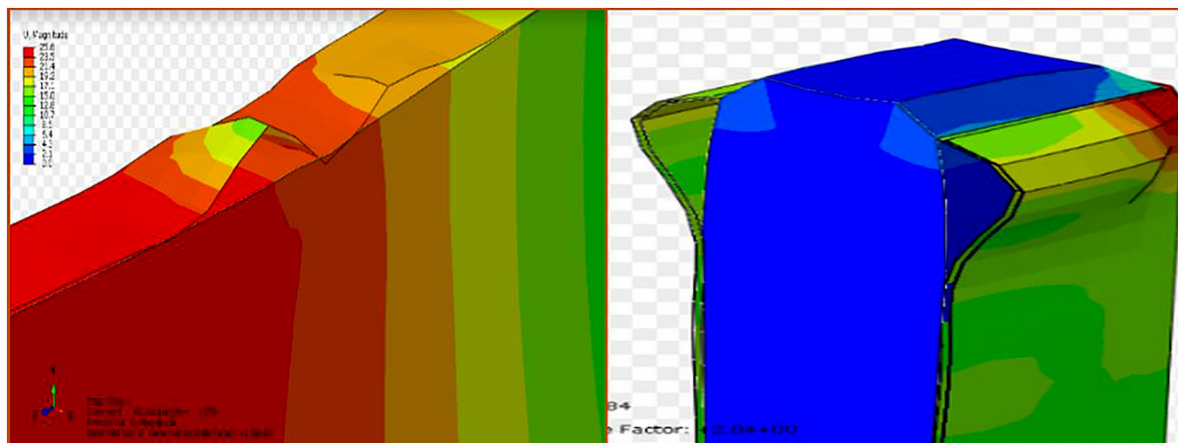


Figure 16: Analysis of beam (a) deformation (b) maximum principal stress (c) maximum elastic stress (d) maximum deformation.

around 0.0031 on the ductile side, which is expected to have some preliminary breakage of concrete. It may also be shown that the mechanical stress in the ultimate bending segments at the tension side is distributed effectively at this phase at the point of center, and the tensile stress of fundamental concrete perpetuates in the ultimate bending segments, with the maximum value of 0.0057 occurring near the load locations at tension end.

The provided information compares experimental and numerical results for the load-carrying capacity of different concrete-filled beams exposed to elevated temperatures (see Table 6). The percentage reductions in load-carrying capacity are as follows:

- M30 grade conventional concrete-filled beam: Experimental reduction of 10%.
- M40 grade conventional concrete-filled beam: Experimental reduction of 15%.
- M20 grade steel fiber-reinforced concrete-filled beam: Experimental reduction of 7%.
- M30 grade steel fiber-reinforced concrete-filled beam: Experimental reduction of 8%.

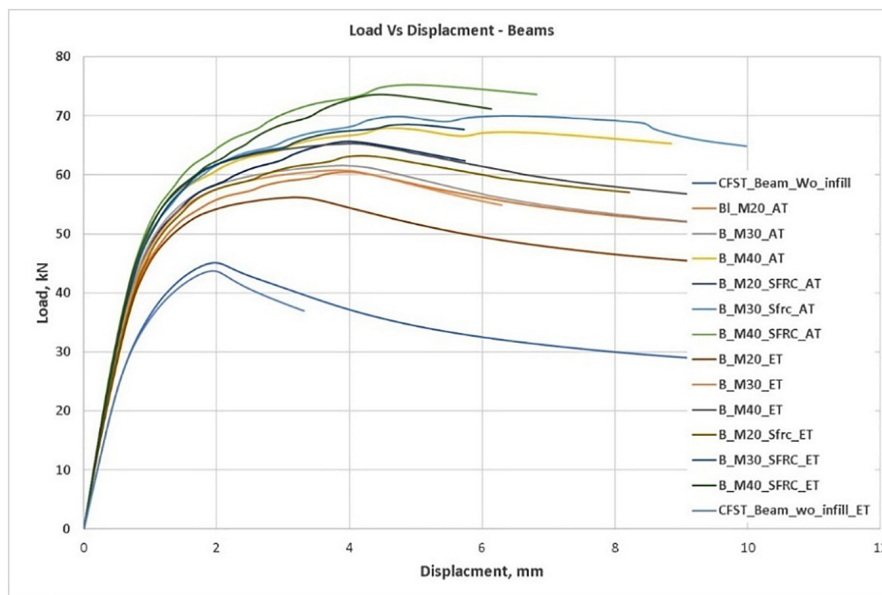


Figure 17: Load vs. displacement in beams.

Table 6: Comparison of experimental and numerical results.

SAMPLE NAME	EXPERIMENTAL RESULTS		NUMERICAL RESULTS	
	MAXIMUM LOAD (kN)	MAXIMUM DEFLECTION (mm)	MAXIMUM LOAD (kN)	MAXIMUM DEFLECTION (mm)
B-AT	42.19	1.98	45.22	2.10
M20-CC-AT1	57.29	4.09	60.63	4.90
B-M20-SFRC-AT2	62.54	4.00	65.72	4.56
B-M30-CC-AT1	59.02	3.97	61.99	4.20
B-M30-SFRC-AT2	67.87	6.35	70.02	7.03
B-M40-CC-AT1	64.43	4.48	67.97	4.99
B-M40-SFRC-AT2	74.89	4.98	78.81	5.69
B-ET	41.34	1.90	43.80	2.02
B-M20-CC-ET1	52.49	3.56	56.56	4.34
B-M20-SFRC-ET2	59.57	4.48	63.76	5.34
B-M30-CC-ET1	57.31	3.89	60.97	4.56
B-M30-SFRC-ET2	65.34	4.99	68.54	6.28
B-M40-CC-ET1	62.76	4.28	65.34	5.04
B-M40-SFRC-ET2	71.51	4.49	73.71	5.45

These reductions represent the decrease in load-carrying capacity observed in the experimental results after exposure to elevated temperatures. It's common to conduct numerical simulations to predict the behavior of structures under different conditions, and in this case, the numerical results are being compared to the experimental findings.

#### 4. CONCLUSIONS

The research objectives aimed to investigate the impact of steel fibers on the load behavior of hollow steel tube beams filled with high-strength concrete. The key findings based on the test results are summarized as follows:

- CFST beams with steel fibers significantly impacted the deformation behavior. Mechanical properties of concrete were highly affected at an elevated temperature of 1050°C, with reductions in mechanical strength, split tensile strength, and flexural strength. This reduction was attributed to the decomposition of calcium hydroxide at elevated temperatures.
- Compared to similar CFST beams without steel fibers, the beams with steel fibers exhibited slightly greater ultimate loads. The inclusion of steel fibers improved the axial load transfer between the CFST hollow steel section and the concrete-filled sections, resulting in increased concrete strength.
- The load-bearing capacity of M20, M30, and M40 grade concrete-filled beams exhibited an increase at both ambient and elevated temperatures, with improvements ranging from 22.5% to 32.5% at ambient temperature and 22.6% to 32.56% at elevated temperature. In contrast, the mechanical properties of modified polymer concrete-filled beams experienced a reduction ranging from 8.2% to 9.8%, while compression strength decreased by 12.85% to 16.23%.
- Furthermore, the experimental load-carrying capacity of the beams is closely aligned with values suggested by various design codes, including EC-EN 1994-1-2005, ANSI/AISC 360-16, AIJ-97, and BS 5950-5-2000. Notably, the EC-EN 1994-1-2005 code demonstrated the highest level of accuracy, with a minimal deviation of approximately 10%. The addition of steel fibers significantly improved the ductility of CFST beams. A minimum of 1% steel fiber volume was found to achieve ductile behavior. This approach was deemed more effective and cost-efficient than increasing the thickness and steel section to enhance the characteristics of CFST beams.
- The use of FEA modeling to investigate the structural capacity of rectangular CFST beams was proposed. The results obtained from the FEA, including anticipated load and deflection, failure mechanisms, and bending capabilities, showed good agreement with experimental findings.
- These findings contribute valuable insights into the behavior and performance of CFST beams with steel fibers, particularly under elevated temperatures, and highlight the effectiveness of steel fibers in enhancing mechanical properties and ductility. The validation of code predictions and the proposed FEA modeling further strengthen the robustness of the study.

#### 5. BIBLIOGRAPHY

- [1] NAKAMURA, S.-I., MOMIYAMA, Y., HOSAKA, T., *et al.*, “New technologies of steel/concrete composite bridges”, *Journal of Constructional Steel Research*, v. 58, n. 1, pp. 99–130, 2002. doi: [http://dx.doi.org/10.1016/S0143-974X\(01\)00030-X](http://dx.doi.org/10.1016/S0143-974X(01)00030-X).
- [2] KANG, J.-Y., CHOI, E.-S., CHIN, W.-J., *et al.*, “Flexural behavior of concrete-filled steel tube members and its application”, *International Journal of Steel Structures*, v. 7, pp. 319–324, 2007.
- [3] ELCHALAKANI, M., ZHAO, X.-L., “Concrete-filled cold-formed circular steel tubes subjected to variable amplitude cyclic pure bending”, *Engineering Structures*, v. 30, n. 2, pp. 287–299, 2008. doi: <http://dx.doi.org/10.1016/j.engstruct.2007.03.025>.
- [4] BAMBACH, M.R., JAMA, H., ZHAO, X.L., *et al.* Hollow and concrete filled steel hollow sections under transverse impact loads”, *Engineering Structures*, v. 30, n. 10, pp. 2859–2870, 2008. doi: <http://dx.doi.org/10.1016/j.engstruct.2008.04.003>.
- [5] TAO, Z., HAN, L.-H., WANG, L.-L., “Compressive and flexural behavior of CFRP-repaired concrete-filled steel tubes after exposure to fire”, *Journal of Constructional Steel Research*, v. 63, n. 8, pp. 1116–1126, 2007. doi: <http://dx.doi.org/10.1016/j.jcsr.2006.09.007>.
- [6] ZHAO, X.-L., ZHANG, L., “State-of-the-art review on FRP strengthened steel structures.”, *Engineering Structures*, v. 29, n. 8, pp. 1808–1823, 2007. doi: <http://dx.doi.org/10.1016/j.engstruct.2006.10.006>.

- [7] GANESH PRABHU, G., SUNDARRAJA, M.C., “Behaviour of concrete filled steel tubular (CFST) short columns externally reinforced using CFRP strips composite.”, *Construction & Building Materials*, v. 47, pp. 1362–1371, 2013. doi: <http://dx.doi.org/10.1016/j.conbuildmat.2013.06.038>.
- [8] TAO, Z., HAN, L.-H., “Behaviour of fire-exposed concrete-filled steel tubular beam-columns repaired with CFRP wraps”, *Thin-walled Structures*, v. 45, n. 1, pp. 63–76, 2007. doi: <http://dx.doi.org/10.1016/j.tws.2006.11.004>.
- [9] PARK, J.W., CHOI, S.M., “Structural behavior of CFRP-strengthened concrete-filled steel tube columns under axial compression loads”, *Steel and Composite Structures*, v. 14, n. 5, pp. 453–472, 2013. doi: <http://dx.doi.org/10.12989/scs.2013.14.5.453>.
- [10] DONG, J.F., WANG, Q.Y., GUAN, Z.W., “Structural behaviour of recycled aggregate concrete filled steel tube columns strengthened by CFRP”, *Engineering Structures*, v. 48, pp. 532–542, 2013. doi: <http://dx.doi.org/10.1016/j.engstruct.2012.11.006>.
- [11] PARK, J., HONG, Y., HONG, G., *et al.*, “Design formulas of concrete-filled circular steel tubes reinforced by carbon fiber reinforced plastic sheets”, *Procedia Engineering*, v. 14, pp. 2916–2922, 2011. doi: <http://dx.doi.org/10.1016/j.proeng.2011.07.367>.
- [12] HU, Y., YU, T., TENG, J., “FRP-confined circular concrete-filled thin steel tubes under axial compression.”, *Journal of Composites for Construction*, v. 15, n. 5, pp. 850–860, 2011. doi: [http://dx.doi.org/10.1061/\(ASCE\)CC.1943-5614.0000217](http://dx.doi.org/10.1061/(ASCE)CC.1943-5614.0000217).
- [13] LIU, L., LU, Y., “Axial bearing capacity of short FRP confined concrete-filled steel tubular columns”, *J Wuhan Univ Technol-Mater Sci Ed*, v. 25, n. 3, pp. 454–458, 2010. doi: <http://dx.doi.org/10.1007/s11595-010-0022-2>.
- [14] TAO, Z., HAN, L.-H., ZHUANG, J.-P., “Axial loading behavior of CFRP strengthened concrete-filled steel tubular stub columns”, *Advances in Structural Engineering*, v. 10, n. 1, pp. 37–46, 2007. doi: <http://dx.doi.org/10.1260/136943307780150814>.
- [15] TENG, J.G., HU, Y.M., YU, T., “Stress–strain model for concrete in FRP-confined steel tubular columns.”, *Engineering Structures*, v. 49, pp. 156–167, 2013. doi: <http://dx.doi.org/10.1016/j.engstruct.2012.11.001>.
- [16] AL ZAND, A.W., BADARUZZAMAN, W.H.W., MUTALIB, A.A., *et al.*, “Finite element analysis of square CFST beam strengthened by CFRP composite material”, *Thin-walled Structures*, v. 96, pp. 348–358, 2015. doi: <http://dx.doi.org/10.1016/j.tws.2015.08.019>.
- [17] SUNDARRAJA, M.C., PRABHU, G.G., “The flexural behaviour of CFST members strengthened using CFRP composites”, *Steel and Composite Structures*, v. 15, n. 6, pp. 623–643, 2013. doi: <http://dx.doi.org/10.12989/scs.2013.15.6.623>.
- [18] WANG, Q.-L., SHAO, Y.B., “Flexural performance of circular concrete filled CFRP-steel tubes”, *Advanced Steel Construction*, v. 11, n. 2, pp. 127–149, 2015.
- [19] WANG, Q.-L., LI, J., SHAO, Y.-B., *et al.*, “Flexural performances of square concrete filled CFRP-steel tubes (S-CF-CFRP-ST)”, *Advances in Structural Engineering*, v. 18, n. 8, pp. 1319–1344, 2015. doi: <http://dx.doi.org/10.1260/1369-4332.18.8.1319>.
- [20] WANG, Z.-B., YU, Q., TAO, Z., “Behaviour of CFRP externally-reinforced circular CFST members under combined tension and bending”, *Journal of Constructional Steel Research*, v. 106, pp. 122–137, 2015. doi: <http://dx.doi.org/10.1016/j.jcsr.2014.12.007>.
- [21] ELCHALAKANI, M., “CFRP strengthening and rehabilitation of degraded steel welded RHS beams under combined bending and bearing”, *Thin-walled Structures*, v. 77, pp. 86–108, 2014. doi: <http://dx.doi.org/10.1016/j.tws.2013.12.002>.
- [22] HAEDIR, J., BAMBACH, M.R., ZHAO, X.-L., *et al.*, “Strength of circular hollow sections (CHS) tubular beams externally reinforced by carbon FRP sheets in pure bending.”, *Thin-walled Structures*, v. 47, n. 10, pp. 1136–1147, 2009. doi: <http://dx.doi.org/10.1016/j.tws.2008.10.017>.
- [23] MILLER, T.C., CHAJES, M.J., MERTZ, D.R., *et al.*, “Strengthening of a steel bridge girder using CFRP plates.”, *Journal of Bridge Engineering*, v. 6, n. 6, pp. 514–522, 2001. doi: [http://dx.doi.org/10.1061/\(ASCE\)1084-0702\(2001\)6:6\(514\)](http://dx.doi.org/10.1061/(ASCE)1084-0702(2001)6:6(514)).
- [24] KIM, Y.J., HARRIES, K.A., “Fatigue behavior of damaged steel beams repaired with CFRP strips”, *Engineering Structures*, v. 33, n. 5, pp. 1491–1502, 2011. doi: <http://dx.doi.org/10.1016/j.engstruct.2011.01.019>.

- [25] GEORGE, C., SELVAN, S.S., “State of Art—Light gauge steel hollow and in-filled columns and beams under elevated temperature”, *Iranian Journal of Science and Technology, Transactions of Civil Engineering*, v. 47, pp. 1265–1276, 2023. doi: <http://dx.doi.org/10.1007/s40996-022-00981-z>.
- [26] LEE, H.H., “Shear strength and behavior of steel fiber reinforced concrete columns under seismic loading”, *Engineering Structures*, v. 29, n. 7, pp. 1253–1262, 2007. doi: <http://dx.doi.org/10.1016/j.engstruct.2006.08.016>.
- [27] WANG, H.T., WANG, L.C., “Experimental study on static and dynamic mechanical properties of steel fiber reinforced lightweight aggregate concrete”, *Construction & Building Materials*, v. 38, pp. 1146–1151, 2013. doi: <http://dx.doi.org/10.1016/j.conbuildmat.2012.09.016>.
- [28] SONG, P.S., HWANG, S., “Mechanical properties of high-strength steel fiber reinforced concrete”, *Construction & Building Materials*, v. 19, n. 9, pp. 669–673, 2004. doi: <http://dx.doi.org/10.1016/j.conbuildmat.2004.04.027>.
- [29] VALLE, M., BUYUKOZTURK, O., “Behavior of fiber reinforced high-strength concrete under direct shear”, *ACI Materials Journal*, v. 90, n. 2, pp. 122–133, 1993.
- [30] KODUR, V.K.R., “Design equations for evaluating fire resistance of SFRC-Filled HSS columns”, *Journal of Structural Engineering*, v. 124, n. 6, pp. 671–677, 1998. doi: [http://dx.doi.org/10.1061/\(ASCE\)0733-9445\(1998\)124:6\(671\)](http://dx.doi.org/10.1061/(ASCE)0733-9445(1998)124:6(671)).
- [31] KODUR, V.K.R., LIE, T.T., “Fire resistance of circular steel columns filled with steel fiber-reinforced concrete”, *Journal of Structural Engineering*, v. 122, n. 7, pp. 776–782, 1996. doi: [http://dx.doi.org/10.1061/\(ASCE\)0733-9445\(1996\)122:7\(776\)](http://dx.doi.org/10.1061/(ASCE)0733-9445(1996)122:7(776)).
- [32] KODUR, V.K.R., “Performance-based fire resistance design of concrete-filled steel columns”, *Journal of Constructional Steel Research*, v. 51, n. 1, pp. 21–36, 1999. doi: [http://dx.doi.org/10.1016/S0143-974X\(99\)00003-6](http://dx.doi.org/10.1016/S0143-974X(99)00003-6).
- [33] KODUR, V.K.R., LIE, T.T., “Fire performance of concrete-filled hollow steel columns”, *Journal of Fire Protection Engineering*, v. 7, n. 3, pp. 89–97, 1995. doi: <http://dx.doi.org/10.1177/104239159500700302>.
- [34] LIE, T.T., CHABOT, M., “A method to predict the fire resistance of circular concrete filled hollow steel columns”, *Journal of Fire Protection Engineering*, v. 2, n. 4, pp. 111–124, 1990. doi: <http://dx.doi.org/10.1177/104239159000200402>.
- [35] CAMPIONE, G., MENDOLA, L.L., SANPAOLESI, L., *et al.*, “Behavior of fiber reinforced concrete-filled tubular columns in compression”, *Materials and Structures*, v. 35, n. 250, pp. 332–337, 2002. doi: <http://dx.doi.org/10.1617/13785>.
- [36] CAMPIONE, G., MINDESS, S., SCIBILIA, N., *et al.*, “Strength of hollow circular steel sections filled with fiber-reinforced concrete”, *Canadian Journal of Civil Engineering*, v. 27, n. 2, pp. 364–372, 2000. doi: <http://dx.doi.org/10.1139/199-079>.
- [37] GOPAL, S.R., MANOHARAN, P.D., “Experimental behaviour of eccentrically loaded slender circular hollow steel columns in-filled with fibre reinforced concrete”, *Journal of Constructional Steel Research*, v. 62, n. 5, pp. 513–520, 2006. doi: <http://dx.doi.org/10.1016/j.jcsr.2005.09.004>.
- [38] ELLOBODY, E., GHAZY, M.F., “Experimental investigation of eccentrically loaded fibre reinforced concrete-filled stainless steel tubular columns”, *Journal of Constructional Steel Research*, v. 76, pp. 167–176, 2012. doi: <http://dx.doi.org/10.1016/j.jcsr.2012.04.001>.
- [39] ELLOBODY, E., “Numerical modeling of fibre reinforced concrete-filled stainless steel tubular columns”, *Thin-walled Structures*, v. 63, pp. 1–12, 2013. doi: <http://dx.doi.org/10.1016/j.tws.2012.10.005>.
- [40] ELLOBODY, E., “Nonlinear behaviour of eccentrically loaded FR concrete-filled stainless steel tubular columns”, *Journal of Constructional Steel Research*, v. 90, pp. 1–12, 2013. doi: <http://dx.doi.org/10.1016/j.jcsr.2013.07.018>.
- [41] TAO, Z., UY, B., HAN, L.H., *et al.*, “Analysis and design of concrete-filled stiffened thin-walled steel tubular columns under axial compression”, *Thin-walled Structures*, v. 47, n. 12, pp. 1544–1556, 2009. doi: <http://dx.doi.org/10.1016/j.tws.2009.05.006>.
- [42] GOPAL, S.R., MANOHARAN, P.D., “Tests on fibre reinforced concrete filled steel tubular columns”, *Steel and Composite Structures*, v. 4, n. 1, pp. 37–48, 2004. doi: <http://dx.doi.org/10.12989/scs.2004.4.1.037>.
- [43] AMERICAN SOCIETY FOR TESTING AND MATERIALS, *ASTM-E8/E8M-09. Standard Test Methods for Tension Testing of Metallic Materials*, West Conshohocken, ASTM, 2009.

- [44] TOKGOZ, S., DUNDAR, C., “Experimental study on steel tubular columns in-filled with plain and steel fiber reinforced concrete”, *Thin-walled Structures*, v. 48, n. 6, pp. 414–422, 2010. doi: <http://dx.doi.org/10.1016/j.tws.2010.01.009>.
- [45] AISC. *Specification for structural steel buildings*. Chicago, AISC, 2010.
- [46] PORTOLÉS, J.M., SERRA, E., ROMERO, M.L., “Influence of ultra-high strength infill in slender concrete-filled steel tubular columns”, *Journal of Constructional Steel Research*, v. 86, pp. 107–114, 2013. doi: <http://dx.doi.org/10.1016/j.jcsr.2013.03.016>.
- [47] Bureau of Indian Standards, *IS 383 (1970): Specification for Coarse and Fine Aggregates, From Natural Sources Concrete*, New Delhi, Bureau of Indian Standards, 1970.
- [48] CHRISTO GEORGE, S., SENTHIL SELVAN, V., SATHISH KUMAR, G., *et al.*, “Enhancing the fire-resistant performance of concrete-filled steel tube columns with steel fiber-reinforced concrete”, *Case Studies in Construction Materials*, v. 20, pp. e02741, 2024. doi: <http://dx.doi.org/10.1016/j.cscm.2023.e02741>.
- [49] EUROPEAN COMMITTEE FOR STANDARDIZATION, *EC4 Design of Composite Steel and Concrete Structures – Part 1. 1: General Rules and Rules for Buildings*, Brussels, European Committee for Standardization; 2004.
- [50] BRITISH STANDARD INSTITUTE, *BS5400-5:1979, Steel, Concrete and Composite Bridges. Part 5: Code of Practice for Design of Composite Bridges*, United Kingdom, British Standard Institute, 1979.
- [51] HATZIGEORGIOU, G.D., BESKOS, D.E., “Minimum cost design of fiber-reinforced concrete-filled steel tubular columns”, *Journal of Constructional Steel Research*, v. 61, n. 2, pp. 167–182, 2005. doi: <http://dx.doi.org/10.1016/j.jcsr.2004.06.003>.
- [52] OLIVEIRA, W.L.A., DE NARDIN, S., EL DEBS, A.L.H.C., *et al.*, “Influence of concrete strength and length/diameter on the axial capacity of CFT columns”, *Journal of Constructional Steel Research*, v. 65, n. 12, pp. 2103–2110, 2009. doi: <http://dx.doi.org/10.1016/j.jcsr.2009.07.004>.